

# Design and testing of a system for measuring high-frequency AC losses in superconducting wires and coils carrying DC and AC currents

Cite as: Rev. Sci. Instrum. 90, 065111 (2019); doi: 10.1063/1.5099559

Submitted: 11 April 2019 • Accepted: 27 May 2019 •

Published Online: 19 June 2019



View Online



Export Citation



CrossMark

Y. Nikulshin,<sup>a)</sup> V. Ginodman, A. Friedman, Y. Yeshurun, and S. Wolfus

## AFFILIATIONS

Institute of Superconductivity, Department of Physics, Bar-Ilan University, Ramat-Gan 5290002, Israel

<sup>a)</sup>Author to whom correspondence should be addressed: [yasha.nick@gmail.com](mailto:yasha.nick@gmail.com)

## ABSTRACT

Development of high-power superconducting applications requires the accurate estimation of AC losses in the superconductor. In applications such as superconducting magnetic energy storage, the charge/discharge/persistent switching frequency of the coil, resulting from pulse width modulation control algorithms, is usually in the kilohertz regime. Therefore, a thorough investigation of the losses in the kilohertz regime of AC currents superimposed on large DC currents is essential in order to ensure the device stable operation at a predefined temperature. We describe here a unique experimental setup designed and built for characterizing AC losses in superconducting wires and coils under such special conditions. To minimize the eddy currents induced in the apparatus, a cryostat vacuum vessel was made of Delrin, an insulating synthetic polymer. The measurement setup allows driving DC currents up to 150 A and superimposed AC currents with amplitudes up to 10 A<sub>rms</sub> and frequencies up to 18 kHz. The system utilizes conduction cooling to reach a wide range of temperatures between 6 and 100 K and allows measurements of 10 cm long superconducting wires and coils with a diameter of 40 cm. The loss is measured by the electrical method, i.e., by direct voltage and current waveform measurement, achieving a resolution better than 100 nW. The system described here will assist in developing superconducting wires and coils for high-power applications.

Published under license by AIP Publishing. <https://doi.org/10.1063/1.5099559>

## I. INTRODUCTION

Estimation of AC losses in superconductors and understanding of their origin are critical for applications. Their importance increases even further when the superconducting device is cooled to its operation temperature by conduction-cooled cryogenfree methods, where a slight imbalance between the heat load and the cooling power may result in a thermal runaway which disables the device operation. Measurements of the AC losses in applications such as Superconducting Magnetic Energy Storage (SMES),<sup>1</sup> Fault Current Limiter (FCL),<sup>2</sup> and High-Voltage DC (HVDC) cables<sup>3</sup> present a unique challenge. In these applications, the superconducting cable or coil carries DC current on which an AC ripple current, resulting from switching, is superimposed. In SMES, for example, the charge/discharge/persistent switching frequency of the coil resulting from Pulse Width Modulation (PWM) control algorithms is usually in the kilohertz regime. Therefore, a thorough investigation of the AC losses in the kilohertz regime is

essential in order to ensure the device stable operation at a predefined temperature.

A common way to measure AC losses is based on the “electrical method”<sup>4,5</sup> in which the current and voltage of the specimen are measured with a lock-in amplifier; the in-phase voltage component represents the losses. This method provides data with relatively high precision and is independent of the cooling approach. Numerous works describing measurements of AC losses in superconducting materials are documented in the literature, see, e.g., Refs. 6–11. However, most of the published studies focus on measurements at relatively low frequencies, usually around the grid frequency, 50–60 Hz and up to 400 Hz.<sup>9,12–15</sup> In addition, to the best of our knowledge, studies of AC losses for AC current superimposed on DC current are hardly available. In addition, while superconducting films, tapes and wires are extensively studied, AC losses in superconducting coils are rarely reported, see, for example, Refs. 16–18. It is the purpose of this article to describe a novel design of a system that enables measuring high-frequency AC losses of superconducting wires and

coils carrying AC currents superimposed on DC currents. The experimental setup described here enables direct electrical measurements of the AC losses in superconducting wires and coils at temperatures between 6 and 80 K, with a loss resolution of 100 nW. The system allows measurements under operation conditions expected in a future SMES application, namely, conduction-cooled specimen, DC currents of 150 A (about 50% of the practical critical current of a wire strand), and relatively small AC ripple currents (up to 8  $A_{rms}$  in our system) and frequency range up to 18 kHz. While motivation for developing this system was measuring AC losses in  $MgB_2$  samples, the system is, of course, not restricted to  $MgB_2$  and can be used for any superconductor with high enough transition temperature,  $T_c$ , such as the pnictides<sup>19</sup> and high- $T_c$  superconductors.<sup>20,21</sup>

In the following, we describe the challenges associated with the design of such an experimental device, and the ways to overcome them. We describe in detail the various parts which compose the system and exhibit some experimental results to demonstrate the capabilities of the system.

## II. INSTRUMENT DESIGN AND DEVELOPMENT

### A. Challenges in system design

In Table I, we summarize the main challenges in designing and building a system for measuring AC losses in superconducting wires and coils resulted from high-frequency AC currents superimposed on large DC current. These challenges stem from the system requirements, namely, a large measurement volume, minimizing eddy currents, superposition of AC-DC current, conduction cooling, and the use of large DC currents transported from room temperature down to cryogenic temperatures.

As the system is made primarily for measuring  $MgB_2$  wires and coils ( $T_c = 39$  K), we set the lowest temperature for the measurement system to around 10 K. Further lowering the setup base temperature seems practically unnecessary because at lower temperatures,  $MgB_2$  shows a high level of flux jumps<sup>22,23</sup> and is less stable. We reach the target temperature by using closed cycle cryocoolers, avoiding the

use of liquid helium and the logistics, and maintenance involved in using it.

### B. Cryostat assembly and cryocoolers

Taking into account the limited cooling power of cryocoolers, we built a multistage conduction-cooled system shown schematically in Fig. 1. The 1st cooling stage is based on an Edwards (0/40) cryocooler. Its purpose is to cool all the wiring which enters the cryostat including the massive current leads. This cryocooler, that has a cooling power of 40 W at 77 K and can reach 30 K without load, absorbs all the heat flowing into the cryostat from the room temperature side through conduction and Ohmic losses in the copper current leads. Parts of the radiation shields described below are also connected to the 1st stage. In equilibrium at 50 K, the 1st cooling stage allows the use of the “cryosaving” technique, namely, current carrying leads made of high temperature superconductors such as BSSCO or YBCO which connect the 1st stage to the 25 K 2nd stage. These leads have two significant advantages. First, they carry the high current to the measured specimen with zero joule heating for DC currents. Second, they reduce significantly the heat flow between the 50 K 1st stage and the 25 K 2nd stage due to the relatively small cross section of the tape. It is important to note, however, that high frequency AC currents do generate heating and AC losses in the high temperature superconductor (HTS) interconnecting cryosavers. To overcome this expected extra heat generation, the HTS tapes are soldered all along with indium to a 0.5 mm thick copper strip that conducts the extra heat to the cryocoolers, 1st and 2nd stages. Of course, while this copper strip increases the thermal stability, it comes with a cost of increasing also the heat flow from the 1st to the 2nd stage and therefore its cross section is minimized. The 2nd stage cools down to 25 K by an Edwards 6/30 cryocooler (6 W at 20 K and 28 W at 77 K). It serves as a middle-point heat sink for the current leads and as a thermal anchor for all the wiring such as thermometers and voltage taps. The thickness of the copper strip soldered to YBCO tape in the current leads between the 2nd and 3rd stages is reduced to 0.1 mm. The 3rd stage utilizes Sumitomo RDK408, a 1 W cooling power at 4 K cryocooler on which the measured specimen is mounted. This

TABLE I. Measurement of system requirements.

Requirement	Challenge
Large volume	Overcome radiation, convection and conduction heat losses using limited cooling power
Minimizing eddy currents	Use of as little as possible metal components while maintaining good thermal conductivity, mechanical strength, and stability
Superposition of AC-DC current	Eliminate ripple effect on DC power supply, avoid cross-talk between AC and DC circuits, clear 50 Hz, and power supply switching frequency and harmonic noises
Conduction cooling	Reach operation temperature lower than 10 K with low cooling power with high temperature homogeneity over the measured wire/coil volume using no copper for mounting support
Current leads of up to 150 A	High inward heat flow to the cryostat due to ohmic and conduction losses in the leads

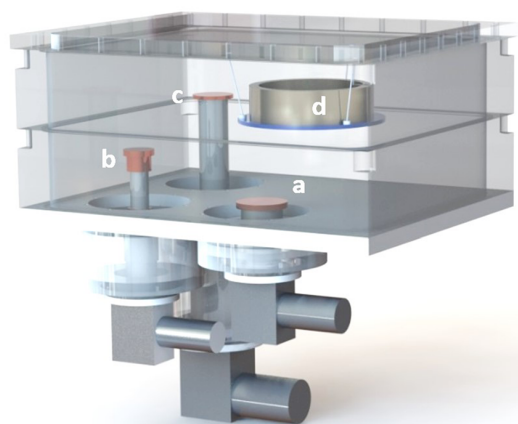


**FIG. 1.** Schematic description of the cryostat assembly. (a) Edwards 0/40, (b) Edwards-6/30, (c) Sumitomo RDK-408D2, and (d) superconducting sample (coil in this scheme).

last cooling stage maintains the temperature of the measured wire or coil.

### C. Eddy currents

In studying AC losses in wires and coils, it is crucial to make sure that the cryogenic surroundings do not affect the measurement. The main source of the possible effect on the AC loss measurements is the loss generated by eddy currents induced in various parts of the cryostat and cryocoolers. In addition, the magnetic field around the specimen can be altered by the eddy currents, contributing to false results. To minimize such artifacts, the use of electrically conductive and/or magnetic materials has to be minimized. For this reason, the whole cryostat enclosure is made of Delrin, an insulating synthetic polymer characterized by its high strength, hardness, and rigidity. The main cryostat body is cut out from two bulks of Delrin material. (The use of two pieces instead of one for the main body was dictated by the limitation of the workshop machinery.) Special care has to be given to sealing the connections between the Delrin plates in order to ensure the vacuum ( $10^{-6}$  Torr) necessary for the measurements. The inner dimensions of the cryostat are 56 cm (width)  $\times$  24 cm (height)  $\times$  44 cm (depth), allowing loss measurement in coils up to 40 cm in diameter. All three cryocoolers are attached to the bottom Delrin plate. The top cover is also made of a Delrin plate. The thickness of each Delrin plate is 25.4 mm. The system is highly scalable. The only limitation for scalability is the vacuum vessel which is harder to manufacture with composite materials due to very large forces. As far as we know, the 2 m OD cryostat made of such materials exists.

The total face area of the cryostat is quite large and requires excellent shielding for minimizing thermal radiation. All internal faces of the cryostat are, therefore, covered with five blankets of multilayer super-insulation (MLI). Each blanket consists of 10 layers of aluminized mica with a weaved spacer in between, 50 layers in total. In addition, an actively cooled radiation shield which is thermally anchored to the 1st stage. We could not use regular copper

sheets as radiation shields because of the expected induced eddy currents. The other common solutions, such as Alumina ( $\text{Al}_2\text{O}_3$ ), Aluminum Nitride (AlN), or Boron Nitride (BN), are not practical because of the high cost involved in shielding the cryostat large area. An innovative solution was implemented to overcome this problem, based on a commercial weaved mesh made of 0.15 mm thick copper wires with 0.25 mm spacing, see Fig. 2. To avoid eddy currents in the mesh loops, we oxidized the mesh, forming a layer of Cu-oxide that coats not only the wire surface but also the overlapping wire junctions. The mesh was sampled at random locations to verify that no electric contact exists between mesh's wires. (The induced eddy currents inside each copper wire have a negligible effect due to the small wire diameter.) We then soldered one end of the mesh blanket to a copper braided cable and anchored to the cryocooler, generating high thermal conductivity in one direction (along the X axis in Fig. 2). Several mesh blankets were used in order to avoid any possible electrical conduction path around the perimeter of the cryostat (i.e., a close loop around the coil). An additional layer of the MLI blanket was thoroughly attached to the copper mesh to screen possible thermal radiation penetrating through the mesh. The problem of eddy currents becomes even more important at locations closer to the specimen (wire or coil). The cooling path to the specimen was therefore made of bulk, hot-pressed Boron Nitride (BN), an electrically nonconductive material with high thermal conductivity (70 W/m K).

### D. Sample holders

A special BN stage was designed for the measured superconducting wires. The stage was placed on a copper plate on top of the 4 K stage cryocooler. To improve thermal contact, the wire was covered with cryogenic thermal grease Apiezon N, mixed with 1  $\mu\text{m}$  boron nitride particles serving as a volume filler. Another piece of BN applies pressure from the top to ensure thermal contact and improve temperature homogeneity. The ends of the wire are soldered with pure indium to the current leads, leaving 80 mm of the wire length free of any metal around. The voltage taps are connected 50 mm apart. Voltage taps are soldered with pure indium as well to minimize thermoelectric effects. The voltage taps are connected in a way that forms "8" shaped loop.<sup>5</sup> This way the pick-up loops are divided into two halves that cancel out the induced voltage

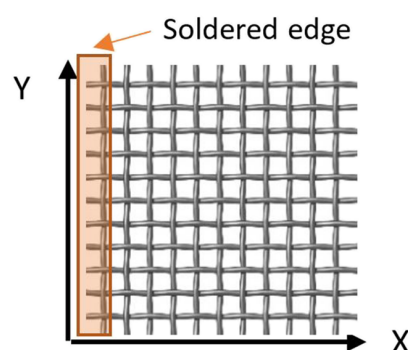


**FIG. 2.** Illustration of a weaved mesh made of 0.15 mm diameter insulated copper wires with 0.25 mm spacing.

picked up by the loop. The distance from the edge of the specimen is at least twice the specimen width. Two  $10\ \Omega$  50 W heaters are attached to the copper plate from both sides of the BN podium. A calibrated silicone diode thermometer is screwed to BN with ceramic bolt and small spring washer to maintain pressure after cool down.

The design is slightly different for measurements of superconducting coils. A 6 mm thick copper plate is connected to the cryocooler [Fig. 3(a)]. The copper plate has a round center hole of 140 mm in diameter and a 5 mm slit for reducing eddy currents. On top of it, a 200 mm diameter and 20 mm thick BN disc is placed. The contact area between the BN disc and the copper plate is  $15\,000\ \text{mm}^2$ , large enough to eliminate any temperature gradients between the surfaces. On top of the BN disc, the coil is placed and pressed against with a fiberglass plate [Fig. 3(b)]. Since the coils had a diameter smaller than the hole in the copper plate, only a small fraction of the flux lines penetrates through the copper. This significantly reduces the eddy currents in the copper plate and therefore improves measurement precision and thermal stability.

### E. Cool down

A vacuum of  $10^{-3}$  Torr was achieved in the Dewar after 10 h of pumping with a conventional rotary vane pump (Edwards 5). Only then, the cryocoolers were started. Due to cryopumping, the pressure dropped to  $10^{-6}$  Torr. The system base temperature is 6 K for short wire samples and 10 K for coils. Recording of the system cool-down process with the sample holder option for short wires measurements is shown in Fig. 4. A steady temperature of 6 K at the sample holder was achieved after 4.5 h. Figure 4 also shows the temperatures measured at the radiation shields at two different locations (A—top cover of the cryostat and B—side wall). Higher measurement temperatures were reached by powering the heaters with proportional–integral–derivative (PID) control algorithm.

### F. Current source

Another important aspect of the measurement system is the current source. As previously mentioned, the SMES operates at a

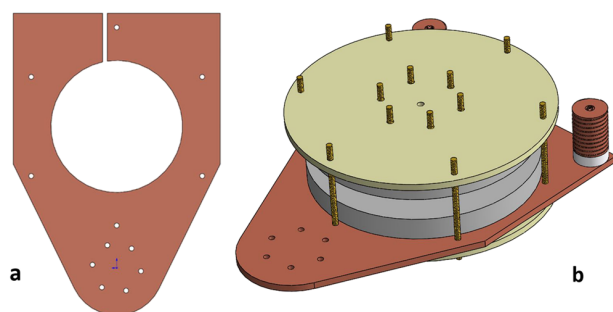


**FIG. 3.** Design of the coil assembly for AC loss measurements (schematic). (a) Copper plate connected to 4.2 K cryocooler and (b) assembled coil with boron nitride former on the copper plate.

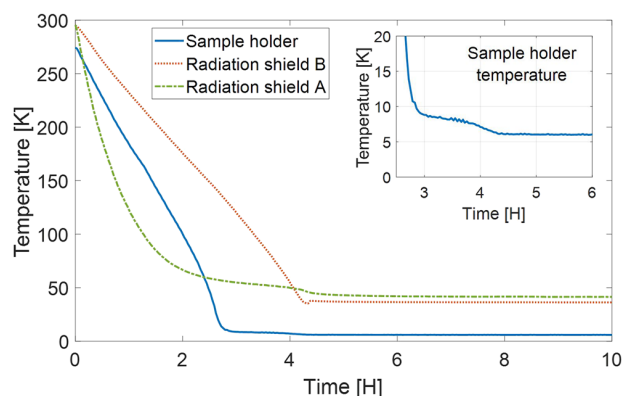


**FIG. 4.** Radiation shield and sample holder temperatures vs time during the cool down of the system with short wire sample. Sample holder (blue solid line), Radiation shields: A—top of the cryostat, B—side wall. Inset: a zoomed-in image of sample holder temperature.

high DC current level accompanied with high frequency AC ripple component. This AC component may be of very low amplitude during compensation charging or be quite significant during discharge. In both cases, the frequency of those AC ripples can be as high as  $10^4$  Hz. To mimic this combination of DC and AC currents flowing through the specimen, a special setup was built. This setup—described schematically in Fig. 5—is capable of driving DC currents of hundreds of amperes alongside AC current with amplitudes ranging from milliamperes to tens of amperes at frequencies up to 18 kHz. The setup is composed of Xantrex power supply, which drives DC currents up to 300 A, a supercapacitor bank of 1000 F connected in parallel, and a homemade air transformer connected in series with its secondary windings to a calibrated noninductive  $0.5\ \text{m}\Omega$  shunt and the measured wire or the coil. The primary side of the air transformer is connected to an AC current source which is basically a signal generator amplified by a professional high-power 6 kW per channel audio amplifier. A  $2\ \Omega$  resistor is required to avoid shorting the amplifier. The DC current also flows through the

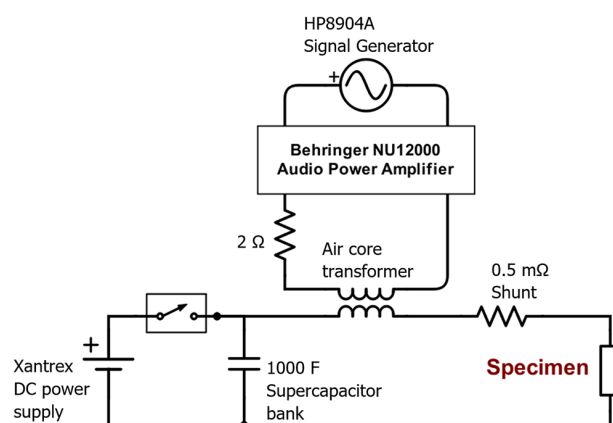


**FIG. 5.** Electrical scheme of the AC/DC current supply for the measurement system.



secondary circuit where the AC current is injected. The DC power supply cannot withstand high AC currents and maintain stable DC current. The supercapacitor bank serves as a bypass route for the AC signal preventing it from flowing through the DC power supply. It also provides a low pass filter for the high frequency switching noise produced by DC power supply. An additional use of the supercapacitors, after being charged and disconnected from DC power supply, is to produce exponential current decay with high enough time constant. This approach mimics the quasi-DC discharge of the SMES. The total resistivity of the loop is  $\sim 30\text{--}40\text{ m}\Omega$  which gives a time constant of  $\sim 40\text{ s}$ . Although the magnetic coupling of air transformer is much worse than in magnetic core based transformers, it is basically the only reasonable option because there is a constant high DC current flowing through the secondary winding which would immediately saturate the magnetic core.

The combination of signal generator and audio power amplifier requires a control based on a feedback loop to set the desired current. The selection of an audio amplifier as an AC current ripple source for the setup was based on its “clean,” low harmonic distortion properties and the audio frequency range (20 Hz–20 kHz), which perfectly matches the required conditions for the experiments.

The pulse nature of PWM waveform introduces copious amounts of high harmonics. High precision current and voltage measurements are, therefore, required for numerically calculating the energy dissipated in the wire. For this purpose, we used a calibrated precision power analyzer PPA-5510 by Newtons 4th. It has an accuracy of 0.01% in voltage, 0.01% in current, and  $0.005^\circ$  in phase measurements. It also allows us to measure harmonics in current and voltage independently up to the 40th harmonic and the total harmonic distortion (THD).

To calibrate the system, we performed a series of measurements using a copper Litz wire sample of 180 strands,  $40\text{ }\mu\text{m}$  each. The use of Litz wire is necessary to avoid additional losses over the DC Ohmic losses, which, in a single filament copper wire, increase with frequency due to the skin effect. With copper Litz wire, we were able to achieve the accurate measurement of  $10\text{ nW} \pm 0.1\text{ nW}$ . However, switching to the superconducting specimen reduced dramatically the measured voltage at low frequencies resulting in an overall measurement resolution of  $100\text{ nW} \pm 2\text{ nW}$ .

### G. Control and data acquisition

All the system instruments are controlled in an MATLAB environment. The developed MATLAB code has graphical user interface (GUI) and all the required automation for the measurements. It also involves a feedback loop for AC and DC currents and a PID for temperature control. The measurement routine scans all the combinations of AC current amplitudes, frequencies, DC currents, and temperatures as defined by the user. It also involves protection algorithms by constantly monitoring the sample temperature and its time derivative to stop the current if the sample is over heated.

### H. Experimental tests

Preliminary measurements of  $\text{MgB}_2$ <sup>24,25</sup> and pnictide wire and tapes<sup>19</sup> were already reported. In Fig. 6, we show typical results for a 36 filamentary  $\text{MgB}_2$  wire with Monel sheath. The wire, with an outer diameter of 1.3 mm, was manufactured by Columbus

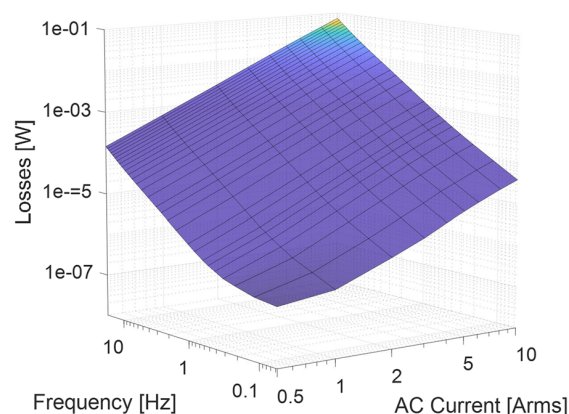


**FIG. 6.** AC loss measurements of 36 filamentary  $\text{MgB}_2$  wire at 10 K, 40 A DC current, frequencies from 57 Hz to 18 kHz, and AC amplitudes from  $0.5\text{ A}_{\text{rms}}$  to  $8\text{ A}_{\text{rms}}$ .

Superconductors.<sup>26</sup> The measurement displayed here was performed at 10 K, 40 A DC current at frequencies up to 18 kHz, and AC amplitudes from  $0.5\text{ A}_{\text{rms}}$  to  $8\text{ A}_{\text{rms}}$ . One can clearly see the losses ranging from lowest values of 100 nW to 0.1 W. Above 100 nW, the measurements are very stable and repetitive.

### III. SUMMARY

We described here a unique experimental setup for measuring AC losses in superconducting wires and coils. The setup focuses on special operation conditions where the superconductor carries high levels of DC current with high-frequency AC current ripple superimposed on it. The system achieves a resolution of 100 nW utilizing a direct voltage and current waveform measurement. To minimize eddy currents within the experimental setup, a special Delrin-made cryostat was designed and built along with a special oxidized copper mesh as active shielding and BN made sample holders. An accurate DC-AC superimposed current was achieved utilizing a supercapacitor bank in DC and AC circuits coupled through an air transformer. The system described here is highly scalable and will assist in developing superconducting wires and coils for high-power applications.

### ACKNOWLEDGMENTS

We thank the faculty mechanical workshop team for its assistance in the system making. The development of the experimental setup was supported by the Israel Ministry of National Infrastructures, Energy and Water. Y.N. acknowledges a Ph.D. Fellowship awarded by the Ministry of Science, Technology and Space.

### REFERENCES

- <sup>1</sup>M. H. Ali, B. Wu, and R. A. Dougal, *IEEE Trans. Sustainable Energy* **1**, 38 (2010).
- <sup>2</sup>J. Bock, M. Bludau, R. Dommerque, A. Hobl, S. Kraemer, M. O. Rikel, and S. Elschner, *IEEE Trans. Appl. Supercond.* **21**, 1202 (2011).

- <sup>3</sup>A. Ballarino, C. E. Bruzek, N. Dittmar, S. Giannelli, W. Goldacker, G. Grasso, F. Grilli, C. Haberstroh, S. Hole, F. Lesur, A. Marian, J. M. Martinez-Val, L. Martini, C. Rubbia, D. Salmieri, F. Schmidt, and M. Tropeano, *IEEE Trans. Appl. Supercond.* **26**, 1 (2016).
- <sup>4</sup>W. J. Carr, *AC Loss and Macroscopic Theory of Superconductors* (CRC Press, Taylor & Francis Group, 2001).
- <sup>5</sup>J. J. Rabbers, B. ten Haken, and H. H. J. ten Kate, *Rev. Sci. Instrum.* **72**, 2365 (2001).
- <sup>6</sup>N. Magnusson, S. Lindau, H. Taxt, and M. Runde, *Supercond. Sci. Technol.* **27**, 105003 (2014).
- <sup>7</sup>Z. Hong, L. Ye, M. Majoros, M. Campbell, and T. Coombs, *J. Supercond. Novel Magn.* **21**, 205 (2008).
- <sup>8</sup>J. Kováč, J. Šouc, P. Kováč, and I. Hušek, *Supercond. Sci. Technol.* **28**, 015013 (2015).
- <sup>9</sup>K. Kajikawa, T. Kawano, R. Osaka, T. Nakamura, M. Sugano, M. Takahashi, T. Wakuda, H. Taxt, N. Magnusson, M. Runde, and S. Brisigotti, *Supercond. Sci. Technol.* **23**, 045026 (2010).
- <sup>10</sup>Y. Nikulshin, Y. Yeshurun, and Y. Wolfus, *Supercond. Sci. Technol.* **32**(7), 075007 (2019).
- <sup>11</sup>J. Kováč, in *MgB<sub>2</sub> Superconducting Wires*, edited by R. Flükiger (World Scientific Publishing Co Pte Ltd., 2016), pp. 419–438.
- <sup>12</sup>J. Kováč, M. Kulich, L. Kopera, and P. Kováč, *Supercond. Sci. Technol.* **31**, 125014 (2018).
- <sup>13</sup>J. Kováč, J. Šouc, and P. Kováč, *Physica C* **475**, 1 (2012).
- <sup>14</sup>J. Jarvela, M. Lyly, A. Stenvall, R. Juntunen, J. Šouc, and R. Mikkonen, *IEEE Trans. Appl. Supercond.* **25**, 1 (2015).
- <sup>15</sup>J. W. Hartwig, B. Fraser, G. Brown, D. Koci, K. R. Hunker, C. Bowman, L. Kohlman, P. Schrum, and D. Matten, in *2018 AIAA/IEEE Electric Aircraft Technologies Symposium* (American Institute of Aeronautics and Astronautics, Reston, Virginia, 2018), pp. 1–24.
- <sup>16</sup>N. Magnusson and S. Hörnfeldt, *Rev. Sci. Instrum.* **69**, 3320 (1998).
- <sup>17</sup>E. Pardo, *Supercond. Sci. Technol.* **26**, 105017 (2013).
- <sup>18</sup>A. Friedman, Y. Wolfus, F. Kopansky, and Y. Yeshurun, *J. Phys.: Conf. Ser.* **234**, 032014 (2010).
- <sup>19</sup>Y. Nikulshin, N. Nechushtan, W. Shuki, Y. Nikulshin, X. Zhang, H. Huang, D. Wang, and M. Yanwei, in *International Conference on Materials and Mechanisms of Superconductivity and High Temperature Superconductors*, Beijing, 2018, p. 599.
- <sup>20</sup>A. Friedman, Y. Wolfus, F. Kopansky, and Y. Yeshurun, *Phys. Procedia* **36**, 1169 (2012).
- <sup>21</sup>D. N. Nguyen, C. H. Kim, J. H. Kim, S. Pamidi, and S. P. Ashworth, *Supercond. Sci. Technol.* **26**, 095001 (2013).
- <sup>22</sup>H. Fujishiro, H. Mochizuki, T. Naito, M. D. Ainslie, and G. Giunchi, *Supercond. Sci. Technol.* **29**, 034006 (2016).
- <sup>23</sup>J. I. Vestgård, T. H. Johansen, A. J. Qviller, T. Qureishy, C. Laliena, P. Mikheenko, R. Navarro, and E. Martínez, *Supercond. Sci. Technol.* **30**, 125005 (2017).
- <sup>24</sup>Y. Nikulshin, S. Wolfus, A. Friedman, V. Ginodman, G. Grasso, M. Tropeano, G. Bovone, M. Vignolo, C. Ferdeghini, and Y. Yeshurun, *IEEE Trans. Appl. Supercond.* **28**, 1 (2018).
- <sup>25</sup>Y. Nikulshin, S. Wolfus, A. Friedman, V. Ginodman, G. Grasso, M. Tropeano, G. Bovone, M. Vignolo, C. Ferdeghini, and Y. Yeshurun, *IEEE Trans. Appl. Supercond.* **28**, 1 (2018).
- <sup>26</sup>See <http://columbussuperconductors.com/> for Columbus Superconductors SPA.